RSC Advances

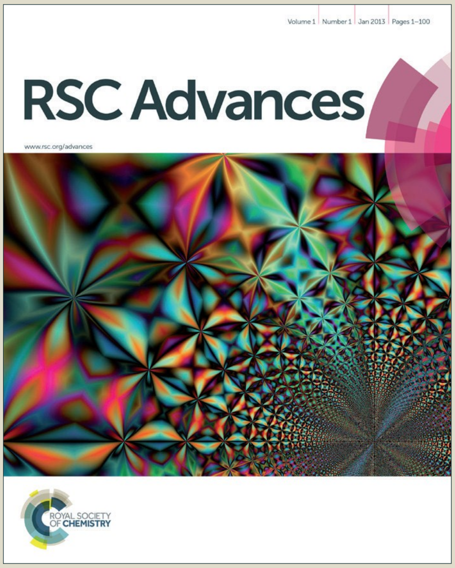

ROYAL SOCIETY OF CHEMISTRY

www.rsc.org/advances

Mechanistic Insights into the Ring-opening of Biomass Derived Lactones

Shelaka Gupta[a], Rishabh Arora[a], Nishant Sinha[b], Md. Imteyaz Alam[a], M. Ali Haider[a*]

[a] *Renewable Energy and Chemicals Laboratory, Department of Chemical Engineering,*
Indian Institute of Technology Delhi, Hauz Khas, New Delhi-110016
[b]*Dassault Systemes, Galleria Commercial Tower, 23 Old Airport Road, Bangalore 560008*
** Corresponding author:*
Tel: +91-11-26591016, Fax: +91-11-2658-2037
E-mail: haider@iitd.ac.in

Abstract— Deoxygenation of biomass-derived lactone molecules such as γ-valerolactone (GVL) by catalytic ring-opening and decarboxylation facilitate the production of a variety of fuels and chemicals. Density functional theory (DFT) calculations were performed to reveal the mechanism of the ring-opening step. In order to elucidate the effect of substituents and ring-size on the rate of the ring-opening step, lactone molecules such as ϒ-butyrolactone (GBL), γ-caprolactone (GCL), δ-valerolactone (DVL) and ε-caprolactone (ECL) were included. DFT calculations show that the ring-opening reaction proceeds via the formation of a stable oxocarbenium intermediate. Subsequently, the ring-opening occurs through a two-step mechanism to yield unsaturated acids. The intrinsic barriers for the two-step reaction in GVL were estimated to be 69 and 48 kJ/mol respectively which are comparable to the experimentally observed apparent activation energy. On changing the ring-size from 5 to 7 member ring lactones (GBL, DVL and ECL), the activation energy for the ring-opening steps was observed to follow the trend as predicted by the strain theory. In contrast, on changing the substituent at C_4 of the 5-member ring lactones (GBL, GVL and GCL), the activation energies for ring-openings are dictated by a combination of inductive and steric effects. It is expected that the stability of the oxocarbenium ion formed will have a significant role on the rate of the ring-opening. The estimated rates for the ring-opening step with respect to the ring-size show a direct correlation with the enthalpy of oxocarbenium ion formation in gas phase. Further investigation by *ab initio* molecular dynamics simulations in implicit and explicit aqueous environment indeed show stable oxocarbenium ion formed which were observed to remain intact for greater than 2 ps of simulation time.

Keywords: *biomass, density functional theory, lactone, oxocarbenium ion, ring-opening.*

1. Introduction

Selective removal of oxygen from biomass derived cyclic oxygenate platform molecules constitutes an essential step in their catalytic transformation to produce a range of biorenewable fuels and chemicals[1,2,3]. Thus, reactions involving ring-opening and decarboxylation of cyclic esters form an effective strategy to achieve this goal[4,5]. Led by the pioneering work of Dumesic and co-workers, numerous studies have reported, γ-valerolactone (GVL) as a potential platform molecule, where one important route of its conversion into linear alkenes involves ring-opening and decarboxylation over an acid catalyst[6]. GVL is produced directly by aqueous phase catalytic processing of biomass derived hexose sugars[7,8]. Similar to GVL, several other lactones[9] such as γ-butyrolactone (GBL), γ-caprolactone (GCL), δ-valerolactone (DVL) and ε-caprolactone (ECL) can be obtained from biomass derived aqueous sugars[10], Figure 1. For example, ECL may be prepared from biomass derived 5-hydroxymethylfurfural (HMF)[11] with high selectivity (>85%)[12]. Biological synthesis route have been reported to produce ECL in high concentration (15.7 g/l) by fed-batch Baeyer-Villiger oxidation of cyclohexanone utilizing recombinant *E.coli*[13]. Similarly, GBL was observed to accumulate in high titer on fermentation of glucose by genetically engineered E.coli[14,15] . A biobased process has been recently patented to convert biomass extract into GBL and DVL[16,17]. Recent work by Mei *et al.* have shown the synthesis of GCL from biomass derived triacetic acid lactone (TAL)[4] . All of these lactone molecules have shown considerable potential to serve as a building blocks and precursors for the production of higher value chemicals, polymers and fuels[18,19,20]. For valorization of these lactone molecules, acid catalyzed ring-opening could form the first and most important step, which has been appropriately emphasized in the study of GVL ring-opening to pentenoic acid and its interconversions[6].

The general reactions of lactone molecule occur via the reactivity of the electrophilic (the ring and carbonyl oxygen) or the nucleophilic (carbonyl and acyl carbon) sites[21,22]. The ring-opening is suggested to proceed through a nucleophilic reaction involving the cleavage of the alkyl or acyl C-O bond[23]. The choice of cleaving bond is decided by nature of the nucleophile[23]. In contrast, in the presence of a Brønsted acid, a proton could very well act as an electrophile and attack to the carbonyl or the ring-oxygen. In this alternative route, the electrophilic addition of a proton may lead to the ring-opening of the lactone via the alkyl C-O cleavage. On the ring-opening of GVL, Dumesic group have suggested the protonation of the cyclic ester to open the ring[24]. However, it remains unclear, whether the protonation constitute an electrophilic addition of the proton to the ring-oxygen or the carbonyl-oxygen. The electrophilic addition of a proton to the carbonyl oxygen leads to the formation of an oxocarbenium ion. Consequently, the oxocarbenium ion ring-opens directly via a nucleophilic water addition to form the alkenoic acid via alkyl C-O cleavage and simultaneous deprotonation from the neighboring carbon. To the best of our knowledge, no study has reported such electrophilic reactions in these lactones, leading to the ring-opening via oxocarbenium ion intermediates. Interestingly, further experiments by Dumesic group using a Lewis acid catalyst such as ϒ-Al_2O_3 shows a significant decrease in the overall yield of the product formed via the ring-opening and decarboxylation of GVL, as compared to the Brønsted acid catalyzed reaction[5]. The product yield was retrieved back on adding tungsten oxide to ϒ-Al_2O_3 catalyst which was due the improvement of the Brønsted acidity of the catalyst. Therefore, the intermediacy of the oxocarbenium ions in the presence of a Brønsted acid could be thought as an important step to have a plausible effect on the overall reactivity.

The formation of oxocarbenium ions is not new to heterocyclic chemistry, where it plays a significant role in important chemical modifications such as furan[25] and glycosidic hydrolysis[26]. Moreover, oxocarbenium ions are reported to form as intermediates or in the transition state structures in several organic reactions which include aldol reaction[27], Prins cyclizations[28], glycosylation[29], acid-mediated additions to acetals[30,31], allyl group transfers[32], and addition of carbonyls to electrophiles[33,34]. Due to their canonical structure, oxocarbenium ions are relatively more stable than the carbenium ion and show significant effect on the reaction rate. Therefore, it is expected that the structure of the oxocarbenium ion formed could possibly explain the observed reaction rates. Herein the ring-opening of the GVL is suggested to proceed via the formation of oxocarbenium ion by *ab initio* density functional theory (DFT) calculations. In order to understand the effect of the substituent and ring-size on the formation of oxocarbenium ion and the rate of the reaction, GBL, GCL, DVL and ECL (as shown in Figure 1) were studied. A strong correlation was envisaged between the stability of the oxocarbenium ion and estimated reactions rates of ring-opening.

2. **Computational Method**

Gradient-corrected DFT calculations as implemented in the $DMol^3$ code by Materials Studio 8.0 (Biovia, San Diego, USA) were used to calculate the reaction energies and activation barriers for different reaction pathways involved in the ring-opening of lactones in the presence of a solvent[35]. The effect of the solvent was simulated using the COSMO (Conductor-like Screening Model), where aqueous solvent is represented by the dielectric constant of water (ε=78.54)[36,37]. The generalized gradient approximation (GGA) corrected with exchange-correlation functional by Perdew-Wang 91 (PW91)[38] was chosen together with the doubled numerical basis set plus polarization basis sets (DNP)[39] and an all–electron basis set. For the geometry optimization, the forces on each atom were converged to less than 0.002 Ha/Å (1 Ha = 2625.5 kJ mol^{-1}). The total energy was converged to less than 1.0×10^{-5} Ha and the displacement convergence was set to less than 0.005 Å. Fermi smearing of 0.005 Ha was used to achieve SCF (Self-Consistent Field) convergence of 1.0×10^{-6} Ha. The choice of the functional (GGA-PW91) was based upon the earlier experience of simulating similar reactions of ring-opening of 2-pyrone molecules in aqueous systems which was performed by the corresponding author of this study[4]. The method was found reliable in calculating activation energies close (±5 kJ/mol) to the experimentally measured value[4]. Similarly, the choice of the basis-set was made from another study on the ring-opening of tetrahydrofuran (THF)[40].

In order to determine the activation barriers for various elementary steps, transition states (TS) were isolated using complete linear synchronous transit/quadratic synchronous transit (LST/QST) approach[41]. In this method, LST maximization is first performed, followed by an energy minimization in directions conjugate to the reaction pathway to obtain the approximated TS, which is used to perform QST maximization, followed by conjugated gradient minimization. The cycle is repeated until a maximum in energy is located. Frequency analysis was utilized to validate the transition state corresponding to single imaginary frequency along the reaction coordinate. Frequency analysis of transition states of representative ring-opening steps are given in Table S1. Atomic charges associated with the transition state or the reactant state were calculated using the Mulliken population analysis method[42].

The rates for the elementary steps associated with the ring-opening reactions were estimated using harmonic transition state theory (TST) calculations[43]. In the statistical mechanical treatment of the TST the rate constant for an elementary step is calculated using frequency of normal modes and energies of the reactant and the TS, given by the following equation[44]:

$$k_{HTST} = \frac{k_B T}{h} . \frac{\Pi_{i=1}^{D}\left(1-e^{-\frac{h\nu_i^*}{k_B T}}\right)}{\Pi_{j=1}^{D-1}\left(1-e^{-\frac{h\nu_j^{\mathrm{int}}}{k_B T}}\right)} . e^{-\frac{(E^*-E^{\mathrm{int}})}{k_B T}}$$

Where, k_B is the Boltzmann constant, h is the Planck's constant, ν_i corresponds to normal mode frequencies, E* is the energy of the transition state and E_{int} is the energy of the reactant state. Symbol * refers to the transition state.

The reactivity of the oxocarbenium ions were correlated with their formation energies in the gas phase for increasing lactones ring-size given by the reaction energy of the following reaction:

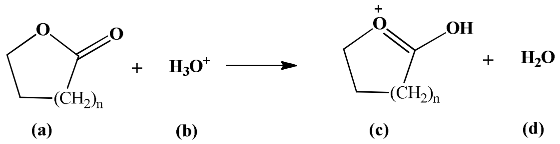

where n represents number of CH_2 unit that could be 1, 2 and 3.

In order to explore the stability of the proposed oxocarbenium ion in aqueous medium, *ab initio* molecular dynamics (AIMD) simulations were carried out with both implicit and explicit solvent models using the $DMol^3$ module in Materials Studio. In the explicit model, the oxocarbenium ion is surrounded by three water molecules that are coordinated to the ion using hydrogen bonds, representing the first solvation shell. The initial structure of this complex was obtained by carving out the ion and the first shell of water molecules around it from the bulk amorphous structure of the ion solvated in water molecules. This bulk amorphous structure, in turn, was obtained using classical molecular dynamics (MD) simulation of a system consisting of the oxocarbenium ion (5.3 wt %) and water molecules. The classical molecular dynamics simulations were carried out for 50 ps using the Forcite module and COMPASS force field. The AIMD simulations, in implicit and explicit models, were carried out for 1 and 5 ps respectively. All molecular dynamics (MD) simulations were carried out within an NVT ensemble (T = 298 K) with a time step of 1 fs. Nose-Hoover thermostat was used to regulate the temperature during the run.

3. Results and Discussion

The first step for GVL conversion to pentenoic acid involves an acid catalyzed ring-opening[2]. The reaction catalyzed by a Brønsted acid catalyst was simulated by the presence of a proton in aqueous environment. The technique of utilizing just a proton in aqueous environment to model the solid acid catalyst, have been successfully implemented in modeling similar reactions of the ring-opening and decarboxylation of 2-pyrones[4]. It is suggested that on ring-opening, GVL forms a carbenium ion which yields pentenoic acid via proton elimination[6]. The DFT simulations for the mechanism of ring-opening of GVL are presented in Figure 2. The Mulliken charge analysis for the solvated GVL is shown in Figure S1. Compared to the ring-oxygen where the partial charge is -0.44 the partial charge on the carbonyl oxygen (-0.5) is higher. Furthermore, the measured energy change for the protonation of the ring oxygen was calculated and found to be of endothermic (+52 kJ/mol) as compared to the protonation on the carbonyl oxygen (-14kJ/mol). Therefore, in the aqueous environment the proton is likely to attack as an electrophile on the carbonyl oxygen as compared to the ring-oxygen. The resultant oxocarbenium ion is highly stable in water with a solvation energy of 14 kJ/mol, Figure 2. It is expected that the oxocarbenium ions are readily formed in water with the aqueous phase shuttling of protons having an activation barrier of around 5.7 kJ/ mol[45]. Thus, the oxocarbenium ion formed in solution serves as a good reference state for comparing the apparent activation barriers in the rest of the discussion. Similar formation of oxocarbenium is reported for Prins cyclization reaction, which involve the coupling of homoallylic alcohols with simple carbonyl compound in presence of Brønsted or Lewis acid catalysts[46] (Figure S2).

The oxocarbenium ion formation leads to the shortening of ring-oxygen and carbonyl carbon i.e. C_1-O bond distance decreases from 1.36 to 1.28 Å. Woods *et al.* observed similar shortening of C-O and C=O bond on the formation of oxocarbenium ion during glycosidic hydrolysis reactions[47]. Therefore, the ring-opening is likely to occur by the cleavage of acyl bond in the aqueous environment to form a carbenium ion (Figure 2, 1a to TS_{1a}) with an intrinsic barrier of 60 kJ/mol. The corresponding transition state structure is shown as TS_{1a} which is product like where an explicit water molecule coordinates with the C_4 to stabilize the carbenium ion formed, resulting in the lowering of activation barrier. Mulliken charge analyses is shown in Figure S3 for the resultant carbenium ion. It is likely that a proton will be abstracted by water from C_3 leading to the formation of the double bond. The intrinsic barrier for the proton elimination step is 76 kJ/mol and the corresponding transition, TS_{1b} is product like. During the hydrogen abstraction by water, a favorable hydrogen bonding interaction with the carbonyl oxygen was observed in the calculation which might have led to the stabilization of the transition state leading to the formation of alkenoic acid. This interaction was observed in the second step of all the reactions studied in this work. An attempt was made to abstract hydrogen without the interaction of water with the carbonyl-oxygen for which a relatively high activation barrier (Ea=210 kJ/mol) was calculated. At 595 K, the enthalpy barrier for the ring-opening of GVL via the two step mechanism were found to be 69 and 48 kJ/mol respectively. The oxocarbenium ion was observed to be more solvated (27 kJ/mol) at higher temperatures as compared to the zero kelvin estimations (14 kJ/mol) as shown in Figure 2(ii). The apparent activation barrier with respect to the reference reactant state for the two-step mechanism was calculated to be 81 kJ/mol (1a' to TS $_{1b'}$, Figure 2 (ii)) which compares well with the experimentally measured value of 85 kJ/mol at 595 K[6]. It is noteworthy that in the absence of significant stabilization of the carbenium ion, a concerted ring-opening may follow in which the proton is eliminated simultaneously from C_3 as the ring opens. The activation barrier for the concerted mechanism is shown in Figure S4 and the estimated ring-opening barriers is of higher value (~200 kJ/mol), which is unlikely to proceed in aqueous solution.

Interestingly, the experimentally measured rate of ring-opening of GVL (20 μmol $min^{-1}g_{cat}^{-1}$) was observed to be similar to GCL (19μmol $min^{-1}g_{cat}^{-1}$)[19]. GVL and GCL differ from each other in terms of the substituent at C_4, which are methyl and ethyl respectively. In order to understand the effect of the substituents at C_4, DFT simulations were performed to study the ring-opening in GBL, GVL and GCL. The corresponding reaction energy diagram for GCL and GBL are shown in Figure 3(i) and (ii) respectively. The ring-opening proceeds in a similar fashion where the oxocarbenium ion ring opens in solution to form a carbenium ion. The solvation energy for the oxocarbenium ion formation were estimated to be 31 and 12 kJ/mol for GCL and GBL respectively, indicating that the substituent at C_4 and increasing carbon length (having no substituent to methyl and ethyl) helps in stabilizing the oxocarbenium ion formation in water. Mulliken charge analysis of the solvated oxocarbenium ions of

GBL, GVL and GCL further supports the trends in solvation energies. The partial positive charge on C_4 of GBL and GVL are 0.107 and 0.112 respectively, which is of similar value, while on the ethyl substituted GCL it is of higher value, 0.123, as shown in Figure S7. Therefore, the oxocarbenium ion of GCL is likely to be more stable in polar solvent such as in water.

The activation energies for the intrinsic step of the ring-opening of GCL as shown in Figure 3(i) (2a to TS_{2a}) was estimated to be similar in value (60 kJ/mol) to the ring-opening step of the GVL (60 kJ/mol) Figure 2, confirming to the experimentally measured rates[19]. On the contrary, the ring-opening of GBL, having no substituent proceeds with slightly lower activation barrier of 56 kJ/mol. It is likely that the positive inductive effect of the ethyl or methyl substituent is responsible for the stabilization of the resultant carbenium ion[19]. However, the methyl or the ethyl substituent may offer a steric hindrance to the water coordination at C_4. Since the transition state is more product-like, it can be hypothesized that the steric effect is dominant over the inductive effect, resulting in the slightly higher estimates of activation barriers for the ring-opening of GCL and GVL as compared to the GBL. This is further supported by experimental studies on GBL where facile ring-opening to γ-hydroxybutyric acid (GHB) is reported in acidic conditions at temperatures as low as 308 K[48]. This observation is further asserted by the studies on lactone polymerization reactions whereon increasing the chain length of alkyl substituents, the polymerization ability of lactones decreases[18]. Similar to GVL, the second step of ring-opening in GBL shows a favorable hydrogen bonding interaction with the carbonyl-oxygen as shown in Figure 3(ii), (3b to TS_{3b}). On the contrary, the hydrogen bonding interaction of the water with the carbonyl-oxygen showed negligible effect on the first step of the ring-opening of the oxocarbenium-ion. In order to elucidate this further, the extra explicit water molecule was positioned to have a favorable hydrogen bonding interaction with the carbonyl-oxygen as shown in Figure S6. The activation barrier of the ring-opening due to this favorable interaction was reduced only by 3 kJ/mol to a value of Ea=53 kJ/mol as compared to the one shown in Figure 3(ii), (3a to TS_{3a}). Thus, this hydrogen bonding interaction is not considered in the first step of the ring-opening in all the reactions studied._The intrinsic barriers for the proton elimination from C_3 resulting in the formation of alkenoic acids in GCL and GBL were calculated to be 65 kJ/mol and 85 kJ/mol respectively as shown in Figure 3 (i) and 3 (ii). Together with GVL the activation energy barrier for proton elimination follows a parallel trend with respect to the increasing carbon length of the substituent showing a clear inductive effect of the methyl and ethyl substituents leading to the stabilization of the carbocations formed in the transition state structures (TS_{2b} and TS_{3b} in Figure 3 and TS_{1b} in Figure 2). The hydrogen atom attached to the C_3 (marked with the yellow color as shown in Figure S3) is likely to be eliminated as compared to the other hydrogen atom attached to the C_3. This is possibly due to the favorable hydrogen bonding interaction of the water with the carbonyl-oxygen which is further supported by Mulliken charge analysis for the intermediate structures 3b, 1b and 2b where an estimate of partial charges on the hydrogen (Figure S3); 0.139, 0.143 and 0.142 indicate the facile elimination from the respective structures.

Experiments by Dumesic group suggest a clear effect of the size of ring on the reactivity of the lactones[19]. In order to understand the effect of ring-size on the ring-opening reaction, DFT calculations were performed for DVL and ECL as shown in Figure 4. Combined with increasing ring-size from GBL to DVL and ECL, it shows a clear trend for the reactivity of 5, 6 and 7-member rings. As predicted by the Baeyer's theory on ring strain, the stability of 6-member cycloalkanes are higher as compared to the 5 and 7-member rings. Between the 5 and 7-member it is difficult to decide the stability, where the 7-member ring is generally greater than or equal to the 5-member ring. While the angular strain is likely to be dominant in 5-member ring, steric strain shows more effect on the stability of the 7-member ring.

The oxocarbenium ion solvation energy for DVL and ECL are estimated to be 44 and 34 kJ/mol, Figure 4(i)(4a) and 4(ii)(5a). Compared to the GBL (Figure 3(ii)(3a)) and ECL, it is evident that the 6-member lactone (DVL) is highly stable in water. The activation barriers for the first step of ring-opening via the formation of oxocarbenium ions of DVL and ECL are calculated as 65 and 66 kJ/mol. These results are further supported by the experimental observations where DVL and ECL showed comparable rates of ring-opening[19]. While the differences in the estimates of activation energies are negligible and within the errors of DFT, the trend in activation energies follows the predictions from strain theory where the 6-member ring requires the highest activation energy for ring-opening. For the second step of hydrogen elimination from C_4 and subsequent alkenoic acid formation, the intrinsic barriers are estimated to be 66 and 74 kJ/mol for DVL and ECL. Primary carbocations are formed as observed in respective transition states (TS_{3b}, TS_{4b} and TS_{5b}) of the three structures with varying chain length of the carboxylic acids of GBL, DVL and ECL. Similar to GVL, a concerted mechanism for the ring-opening and simultaneous hydrogen elimination from the neighboring carbon was considered for 6-member ring DVL. However, it showed significantly higher activation energy (~233 kJ/mol), Figure S5. We have therefore considered the two-step mechanism as the most favorable route for ring-opening of lactones in aqueous systems. Overall activation barrier follows the order GBL (91 kJ/mol)>DVL (84kJ/mol) >ECL (78 kJ/mol).

A possible relationship between the gas phase oxocarbenium ion formation energy and rate of the ring-opening step can be envisaged with respect to the change in ring-size. Figure 5 shows a linear plot for the increase in the rate of the ring-opening step with the decrease in the oxocarbenium-ion formation energy for the 5, 6 and 7-member lactones; GBL, DVL and ECL. Following the strain theory, 6-member oxocarbenium was observed to be more stable and less reactive as compared to the 5 and 7-member ring. The rate of the ring-opening for the GBL is estimated to be higher as compared to ECL, possibly due to the strain and lower heat of combustion in ECL[49]. A more comprehensive relationship between the reaction rate and oxocarbenium ion formation energy has been proposed for the C-O hydrogenolysis reactions in biomass derived cyclic ethers and polyols[50]. Such an understanding could also be developed on a variety of lactone molecules by measuring the experimental rates of ring-opening, which will be the part of a future communication. Nevertheless, the role of the stability of oxocarbenium ions in determining the rates of the subsequent ring-opening is emphasized in these calculations.

The oxocarbenium ion intermediates are difficult to detect by experiments due to its short life time[47]. Studies on glycoside hydrolysis have shown that the oxocarbenium ions are often not solvent equilibrated and their lifetime is relatively short, of the order of 1 to 3 ps[51]. For a reaction to proceed via an oxocarbenium ion intermediate, the half-life of the oxocarbenium ion intermediate should be significantly greater than the bond vibrations which are of the order of 10^{-13} sec[52]. The rate constants for the hydration of the oxocarbenium ions of glycosyl was estimated to be the order of 10^{12} sec^{-1} which is considered to be significant for its formation as an intermediate[52]. On the contrary, the rate constant for the hydration of the methoxymethyl oxocarbenium ions is estimated to be the order of 10^{15} sec^{-1} which may result in negligible barrier to its formation as an intermediate in aqueous systems[52]. Therefore, it is desirable to study the stability and life-time of the oxocarbenium ion formation in aqueous system for the lactones ring-opening reactions. AIMD simulations were performed for 1 and 5 ps of the simulations time in implicit and explicit solvation models respectively and the results are shown in Figure 6 (i) and 6 (ii) respectively. The implicit continuum model shows that the oxocarbenium ions remained stable for 1ps, Figure 6 (i)(a to d). In explicit water environment, simulations were performed with three water molecules, which were coordinated with the oxocarbenium ion by hydrogen bonding interactions. Figure 6 (ii)(a to d) shows the snapshots at 1 ps, 1.5 ps, 3.5 ps and 4.86 ps. Figure 6(iii) shows the distance of nearest hydrogen to carbonyl oxygen versus time. It is observed that for the initial time period of simulation and up to 2.5 ps, the proton was attached to the carboxyl oxygen forming the oxocarbenium ion, Figure 6 (iii). The proton shuttling between water and the carbonyl oxygen started occurring for time periods, over and above 2.5 ps and the proton was visualized mostly in the solvent medium at 3.5 ps. A snapshot of 4.86 ps, show that the proton is back to the carbonyl oxygen, Figure 6 (ii)(d). These results establish the likelihood of oxocarbenium ion intermediate formation in the aqueous solutions for lactones ring-opening reaction[52].

Experimental studies for ring-opening and decarboxylation of GVL on Υ-Al_2O_3 have shown a significant decrease in the C_4 (butene) product yield (~43 %) as compared to the Brønsted acid (SiO_2/Al_2O_3) catalyzed reaction, where the yield was measured to be as high as 92%[5]. Tungsten oxide (WO_x) addition significantly increases the Brønsted acidity of the Υ-Al_2O_3 catalyst. On adding 20 wt% WO_x to Al_2O_3, C_4 product yield was observed to be as high as 80%[5]. In a thesis work, Neurock and co-workers have studied the Lewis acid mediated ring-opening and decarboxylation of GVL on the Υ-Al_2O_3 surface[53]. The activation barrier for ring-opening was calculated to be significantly higher (115 kJ/mol) as compared to the hydride shift (E_a = 54 kJ/mol) and decarboxylation (E_a = 67 kJ/mol) of the resultant carbenium ion[53]. These results further emphasize the importance of the likely rate-determining ring-opening step in the overall conversion of GVL to butene (C_4) isomers. In the absence of a proton, the ring-opening is mediated by the Lewis acid sites, leading to the direct formation of the carbenium ion. The direct ring-opening route having a significantly high activation barrier of ring-opening may possibly explain the lesser C_4 product yield. However, on introducing Brønsted acidity to the Υ-Al_2O_3 catalyst by adding 20 wt% WO_x, oxocarbenium ions are likely to form as an intermediate facilitating the ring-opening on the surface of Υ-Al_2O_3. Oxocarbenium ions formation in aqueous solution in the presence of a Brønsted acid may provide a clue to the measured high yield of the product. Deducing from the DFT simulation results of this study, it can be asserted that the oxocarbenium ion intermediates formed in presence of a Brønsted acid lead to higher rates of ring-opening in aqueous solutions, as compared to the Lewis acid catalyzed reactions. This hypothesis, however, needs to be explored in detail by performing similar simulations on the catalyst surface.

4. Conclusions

DFT simulations predicted the formation of oxocarbenium ions in the acid catalyzed ring-opening of lactones to alkenoic acids. The ring-opening proceeds in two steps where oxocarbenium ion ring-opens to form stable carbenium ions, which on subsequent hydrogen elimination from the neighboring carbon leads to the formation of alkenoic acid. In an alternative route, a concerted mechanism for the ring-opening of the oxocarbenium ion was considered, however it was calculated to show significantly higher activation barrier as compared to the proposed two-step mechanism. A variety of lactone molecules with the change in alkyl substituents at C_4 (GBL, GVL and GCL) and ring-size (GBL, DVL and ECL) were included in the study. The activation barriers estimated for these lactones show a clear trend as predicted by strain theory, inductive and steric effects. The oxocarbenium ion formation energy in gas phase of the lactone molecule with increasing ring-size show an approximately linear relationship with the rate of ring-opening step in aqueous solutions. These observations emphasize the important role of oxocarbenium ions formed in determining the reaction rate. AIMD simulations conducted for 1 to 5 ps in implicit and explicit water environments confirms to the stability of oxocarbenium ion, which makes it likely to be formed as an intermediate in lactones ring-opening reaction.

Acknowledgement

The authors would like to acknowledge the help provided by Dr. Manish Agarwal in the Computer Service Centre at IIT Delhi in setting up the calculations. Shelaka Gupta and Rishabh Arora have equally contributed in this study. We acknowledge the financial support from the Department of Biotechnology (BT/COE/34/SP15097/2015), Government of India to carry out this work.

References

1. Lin, Y.C. & Huber, G. W. The critical role of heterogeneous catalysis in lignocellulosic biomass conversion. *Energy Environ. Sci.* **2,** 68 (2009).

2. Alonso, D. M., Bond, J. Q. & Dumesic, J. A. Catalytic conversion of biomass to biofuels. *Green Chem.* **12,** 1493–1513 (2010).

3. Bardhan, S. K., Gupta, S., Gorman, M. E. & Haider, M. A. Biorenewable chemicals: Feedstocks, technologies and the conflict with food production. *Renew. Sustain. Energy Rev.* **51,** 506–520 (2015).

4. Chia, M., Haider M.A., Pollock G., Kraus G.A., Neurock M. & Dumesic J.A. Mechanistic Insights into Ring-Opening and Decarboxylation of 2-Pyrones in Liquid Water and Tetrahydrofuran. *J. Am. Chem. Soc.* **135,** 5699–5708 (2013).

5. Wang, D., Hakim, S. H., Alonso, D. M. & Dumesic, J. A. A highly selective route to linear alpha olefins from biomass-derived lactones and unsaturated acids. *Chem. Commun.* **49,** 7040–7042 (2013).

6. Bond, J. Q., Wang, D., Alonso, D. M. & Dumesic, J. A. Interconversion between γ-valerolactone and pentenoic acid combined with decarboxylation to form butene over silica/alumina. *J. Catal.* **281,** 290–299 (2011).

7. Braden, D. J., Henao, C. A., Heltzel, J., Maravelias, C.C. & Dumesic, J. A. Production of liquid hydrocarbon fuels by catalytic conversion of biomass-derived levulinic acid. *Green Chem.* **13,** 1755 (2011).

8. Son, P. A., Nishimura, S. & Ebitani, K. Production of γ-valerolactone from biomass-derived compounds using formic acid as a hydrogen source over supported metal catalysts in water solvent. *RSC Adv.* **4,** 10525 (2014).

9. Shi, Z.R., Shen Y.H., Zhang X.Y., Fang Xin., Zeng R.T., Liu Q.X. *et al.* . *RSC Adv.* **5,** 91640–91644 (2015).

10. Isikgor, F. H. & Becer, C. R. Lignocellulosic biomass: a sustainable platform for the production of bio-based chemicals and polymers. *Polym. Chem.* **6,** 4497–4559 (2015).

11. Alam, Md.I., De S., Dutta, S. & Saha, B. Solid-acid and ionic-liquid catalyzed one-pot transformation of biorenewable substrates into a platform chemical and a promising biofuel. *RSC Adv.* **2,** 6890 (2012).

12. Buntara T., Noel S., Phua P.H., Cabrera I.M., Vries J.G. & Heeres H.J. Caprolactam from Renewable Resources: Catalytic Conversion of 5-Hydroxymethylfurfural into Caprolactone. *Angew. Chemie Int. Ed.* **50,** 7083–7087 (2011).

13. Lee, W., Park, E. & Kim, M. Enhanced production of ε-caprolactone by coexpression of bacterial hemoglobin gene in recombinant Escherichia coli expressing cyclohexanone monooxygenase gene. *J. Microbiol. Biotechnol.* **24,** 1685–1689 (2014).

14. Yim, H., Haselbeck R., Niu W., Baxley C.P., Burgard A., Boldt J. *et al.* Metabolic engineering of Escherichia coli for direct production of 1,4-butanediol. *Nat Chem Biol* **7,** 445–452 (2011).

15. Hwang, D. W., Kashinathan P., Lee J.M., Lee J.H., Lee U.H., Hwang J.S. *et al.* Production of γ-butyrolactone from biomass-derived 1,4-butanediol over novel copper-silica nanocomposite. *Green Chem.* **13,** 1672 (2011).

16. Walsem, J.V., Anderson E., Licata J., Sparks K.A., Mirley C., Sivasubramanian M.S. Process for producing a monomer component from a genetically modified polyhydroxyalkanoate biomass. (2012). U.S. Patent 0315681, 2012.

17. Zhuang, Q., Wang, Q., Liang, Q. & Qi, Q. Synthesis of polyhydroxyalkanoates from glucose that contain medium-chain-length monomers via the reversed fatty acid β-oxidation cycle in Escherichia coli. *Metab. Eng.* **24,** 78–86 (2014).

18. Saiyasombat, W., Molloy R., Nicholson T.M., Johnson A.F., Ward I.M. & Poshyachinda S. Ring strain and polymerizability of cyclic esters. *Polym. Pap.* **39,** 5581–5585 (1998).

19. Bond, J. Q., Martin Alonso, D., West, R. M. & Dumesic, J. A. γ-Valerolactone Ring-Opening and Decarboxylation over SiO_2/Al_2O_3 in the Presence of Water†. *Langmuir* **26,** 16291–16298 (2010).

20. Zeng, T., Qian, Q., Zhao, B., Yuan, D., Yao, Y., & Shen, Q. Synthesis and characterization of rare-earth metal guanidinates stabilized by amine-bridged bis(phenolate) ligands and their application in the controlled polymerization of rac-lactide and rac-β-butyrolactone. *RSC Adv.* **5,** 53161–53171 (2015).

21. N Nicolás-Vázquez, I., Méndez-Albores, A., Moreno-Martínez, E., Miranda, R. & Castro, M. Role of Lactone Ring in Structural, Electronic, and Reactivity Properties of Aflatoxin B1: A Theoretical Study. *Arch. Environ. Contam. Toxicol.* **59,** 393–406 (2010).

22. Liotta, D. & Santiesteban, H. Nucleophillic ring opening of lactones via S_N2-type reaction with uncomplexed phenyl selenide anion. *Tetrahedron Lett.* 4369–4372 (1977).

23. Albertsson, A. & Varma, I. K. Recent Developments in Ring Opening Polymerization of Lactones for Biomedical Applications. *Biomacromolecules* **4,** 1466–1486 (2003).

24. Bond, J. Q., Alonso, D. M., Wang, D., West, R. M. & Dumesic, J. A. Integrated catalytic conversion of gamma-valerolactone to liquid alkenes for transportation fuels. *Science* **327,** 1110–4 (2010).

25. Nimlos, M. R., Qian, X., Davis, M., Himmel, M. E. & Johnson, D. K. Energetics of Xylose Decomposition as Determined Using Quantum Mechanics Modeling. *J. Phys. Chem. A* **110,** 11824–11838 (2006).

26. Denekamp, C. & Sandlers, Y. Formation and stability of oxocarbenium ions from glycosides. *J. Mass Spectrom.* **40,** 1055–63 (2005).

27. Kanwar, S. & Trehan, S. Acetate aldol reactions of chiral oxocarbenium ions. *Tetrahedron Lett.* **46,** 1329–1332 (2005).

28. Olier, C., Kaafarani, M., Gastaldi, S. & Bertrand, M. P. Synthesis of tetrahydropyrans and related heterocycles via prins cyclization; extension to aza-prins cyclization. *Tetrahedron* **66,** 413–445 (2010).

29. Zechel, D. L. & Withers, S. G. Glycosidase Mechanisms : Anatomy of a Finely Tuned Catalyst. *Acc. Chem. Res.* **33,** 11–18 (2000).

30. Sammakia, T. & Smith, R. S. Direct evidence for an oxocarbenium ion intermediate in the assymetric cleavage of chiral acetals. *J. Am. Chem. Soc.* **114,** 10998–10999 (1992).

31. Smith, A. B., Fox, R. J. & Razler, T. M. Evolution of the Petasis - Ferrier union/rearrangement tactic : construction of architecturally complex natural products possessing the ubiquitous cis-2,6-substituted tetrahydropyran structural element . *Acc. Chem. Res.* **41,** 675–687 (2008).

32. Nokami, J., Ohga M., Nakamoto H., Matsubara T., Hussain I. & Kataoka K. The first and highly enantioselective crotylation of aldehyde via an allyl transfer reaction from a chiral crotyl donor. *J. Am. Chem. Soc.* **123,** 9168–9169 (2001).

33. Va, H., Ballesteros, A., Gonza, M., V, O. & Cla, V. Cyclization of Carbonyl Groups onto alkynes upon reaction with IPy 2 BF 4 and their trapping with nucleophiles : a versatile trigger for assembling oxygen heterocycles. *J. Am. Chem. Soc.* **125,** 9028–9029 (2003).

34. Pohlhaus, P.D., Sanders S.D., Parsons A.T., Li W. & Johnson J.S. Scope and mechanism for lewis acid-catalyzed cycloadditions of aldehydes and donor - acceptor cyclopropanes : evidence for a stereospecific intimate ion pair pathway. *J. Am. Chem. Soc.* **130,** 8642–8650 (2008).

35. Delley, B. From molecules to solids with the DMol^3 approach. *J. Chem. Phys.* **113,** 7756 (2000).

36. Klamt, A. & Schuurmann, G. COSMO: a new approach to dielectric screening in solvents with explicit expressions for the screening energy and its gradient. *J. Chem. Soc. Perkin Trans. 2* 799–805 (1993).

37. Andzelm, J., Kölmel, C. & Klamt, A. Incorporation of solvent effects into density functional calculations of molecular energies and geometries. *J. Chem. Phys.* **103,** 9312 (1995).

38. Perdew, J. P. & Wang, Y. Accurate and simple analytic representation of the electron-gas correlation energy. *Phys. Rev. B* **45,** 244–249 (1992).

39. Delley, B. Ground-State Enthalpies : Evaluation of electronic structure approaches with emphasis on the density functional method. *J. Phys. Chem. A* **110,** 13632–13639 (2006).

40. Buntara, T., Cabrera I.M., Tan Q., Fierro J.L.G., Neurock M., Vries J.G. *et al.* Catalyst studies on the ring opening of tetrahydrofuran – dimethanol to 1,2,6-hexanetriol. *Catal. Today* **210,** 106–116 (2013).

41. Halgren, T. A. & Lipscomb, W. N. The synchronous-transit method for determining reaction pathways and locating molecular transition states. *Chem. Phys. Lett.* **49,** 225–232 (1977).

42. Mulliken, R. S. Electronic Population Analysis on LCAOMO Molecular Wave Functions. I. *J. Chem. Phys.* **23,** 1833 (1955).

43. Delph, T. J., Cao, P., Park, H. S. & Zimmerman, J. A. A harmonic transition state theory model for defect initiation in crystals. *Model. Simul. Mater. Sci. Eng.* **21,** 025010 (2013).

44. Vinbyard, H. Frequency factors and isotope effects in solid state rate processes. *J. Phys. Chem. Solids* **3,** 121–127 (1957).

45. Laria, D. & Ciccotti, G. Activation free energy for proton transfer in solution. *Chem. Phys.* **180,** 181–189 (1994).

46. Han, X., Peh G.R. & Floreancig, P.E. Prins-type cyclization reactions natural product synthesis. *European J. Org. Chem.* **2013,** 1193–1208 (2013).

47. Woods, R. J., Andrews, C. W. & Bowen, J. P. Molecular mechanical investigations of the properties of oxocarbenium ions. 1. Parameter development. *J. Am. Chem. Soc.* **114,** 850–858 (1992).

48. Pe, M. T., Manso, A., Garcı, M. P., Calle, E. & Casado, J. Reactivity of lactones and GHB Formation. *J. Org. Chem.* **70,** 420–426 (2005).

49. Morrison, R. T. & Boyd R.N. *Organic Chemistry*. 1–1279 (2002).

50. Chia, M., Pagan-Torres Y.J., Hibbitts D., Tan Q., Pham H.N., Datye A.K. *et al*. Selective Hydrogenolysis of Polyols and Cyclic Ethers over Bifunctional Surface Sites on Rhodium-Rhenium Catalysts. *J. Am. Chem. Soc.* **133,** 12675–12689 (2011).

51. Stubbs, J. M. & Marx, D. Glycosidic bond formation in aqueous solution : on the oxocarbenium intermediate. *J. Am. Chem. Soc.* **125,** 10960–10962 (2003).

52. Amyes, T. L. & Jencks, W. P. Lifetimes of oxocarbenium ions in aqueous solution from common ion inhibition of the solvolysis of a-Azido ethers by added azide ion. *J. Am. Chem. Soc.* **111,** 7888–7900 (1989).

53. Marranca, J. Theoretical insights into the conversion of gamma-valerolactone to butene over gamma-alumina. 1–48 (2014). M.S. Thesis, University of Virginia. 1–48 (2014) at http://libra.virginia.edu/catalog/libra-oa:7809.

List of Figures:

Figure No.	Title
Figure 1.	Routes for the synthesis of biomass derived lactone molecules included in this study: ε-caprolactone (ECL), γ-valerolactone (GVL), *γ-caprolactone* GCL, γ -butyrolactone (GBL) and δ-valerolactone (DVL).
Figure 2.	DFT calculated energy diagram for GVL ring-opening to pentenoic acid.
Figure 3.	DFT calculated energy diagram for the ring-opening of (i) GCL to form hex-3-en-oic acid and (ii) GBL to form but-3-en-oic acid.
Figure 4.	DFT calculated energy diagram for the ring-opening of (a) DVL to form pent-4-en-oic acid and (b) ECL to form hex-3en-oic acid.
Figure 5.	Reaction rate constant for ring-opening of lactone molecules versus the respective gas-phase oxocarbenium ion formation energies.
Figure 6.	AIMD simulation of the oxocarbenium ion of GVL in (i) implicit and (ii) explicit water environment. (iii) Nearest hydrogen distance from carbonyl oxygen of GVL during ab initio MD simulation in explicit water.

Figure 1

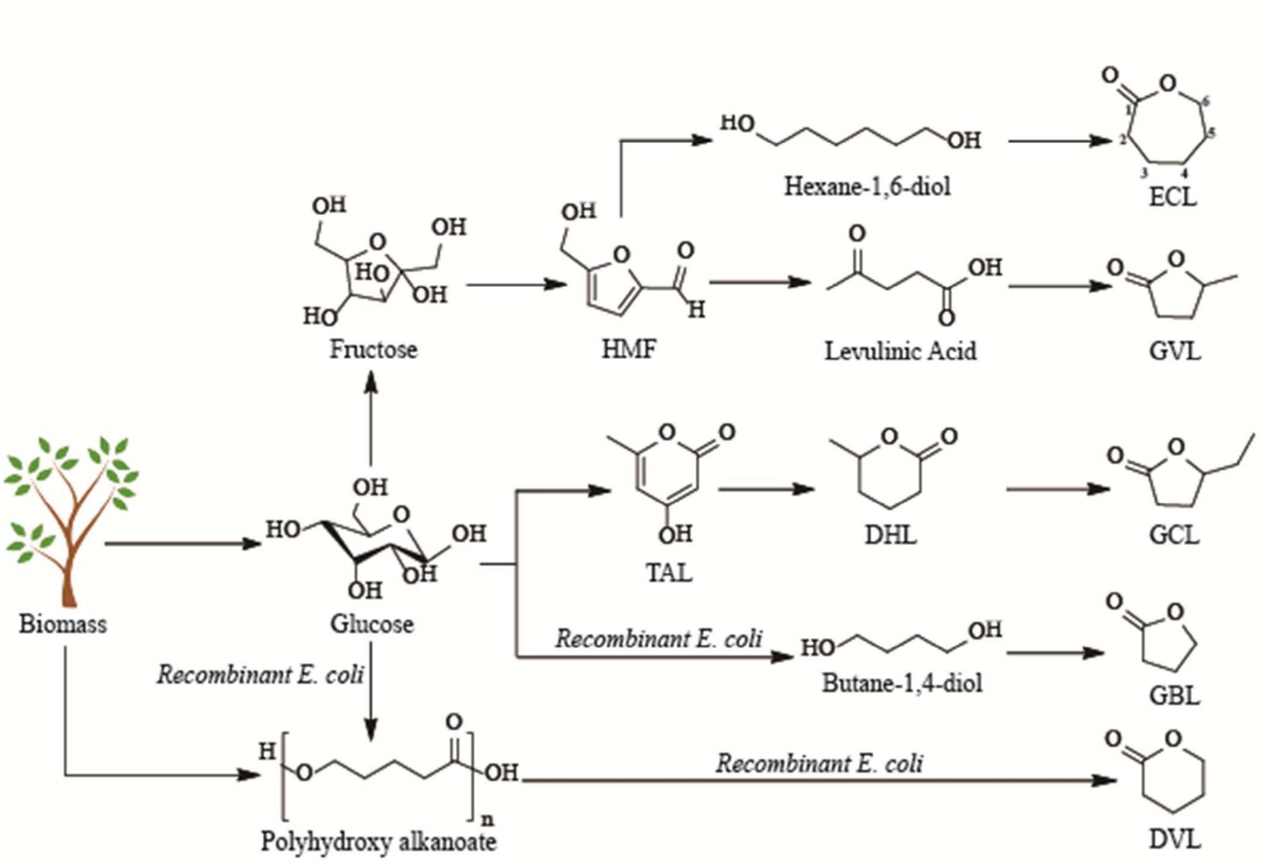
Hexane-1,6-diol
ECL
Fructose
HMF
Levulinic Acid
GVL
Biomass
Glucose
TAL
DHL
GCL
Recombinant E. coli
Butane-1,4-diol
GBL
Recombinant E. coli
Polyhydroxy alkanoate
Recombinant E. coli
DVL

Figure 2

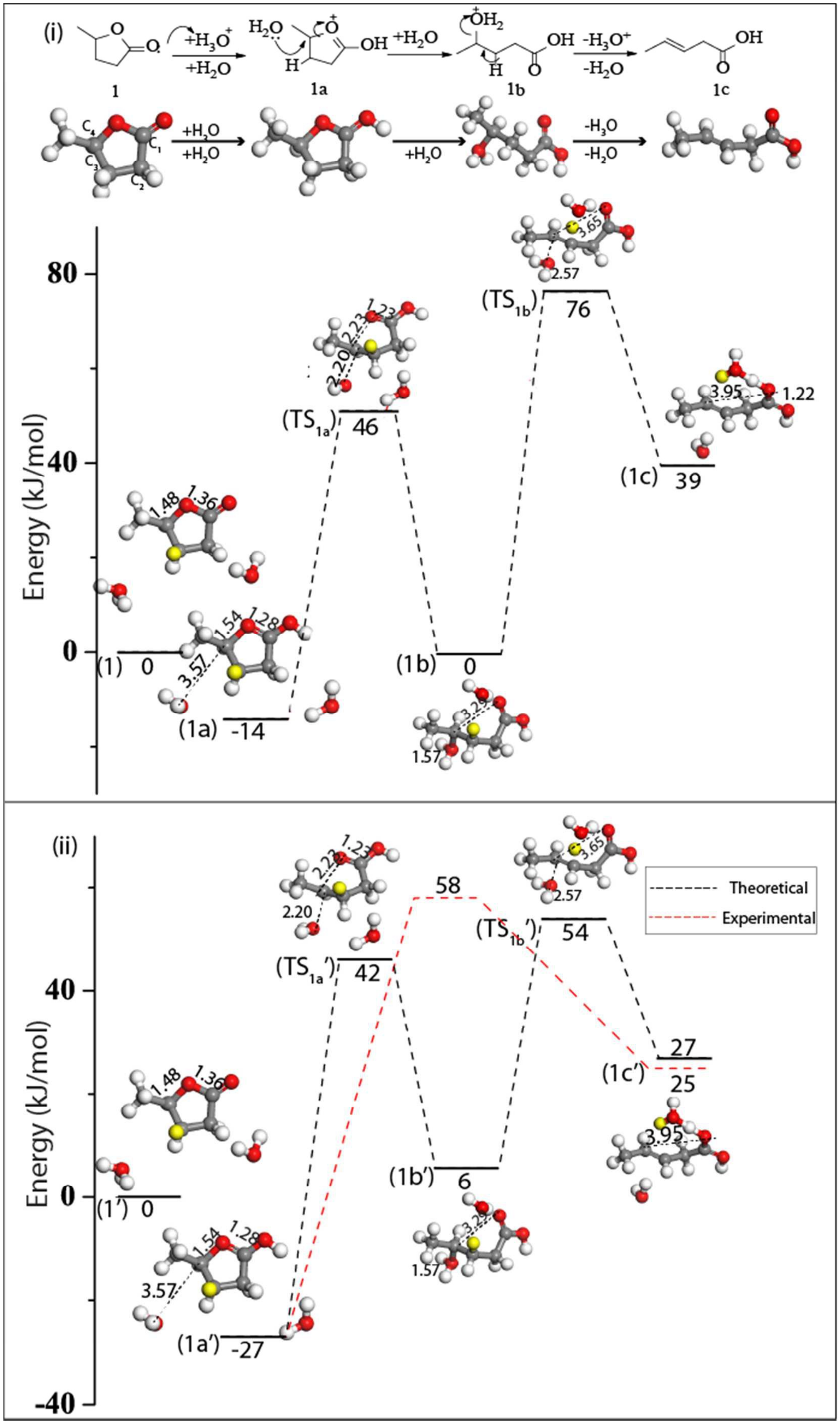
(i)
+H3O+
+H2O
H2O
OH
+H2O
OH2
-H3O+
-H2O
1
1a
1b
1c
C4
C1
C3
C2
+H2O
+H2O
-H3O
-H2O
Energy (kJ/mol)
80
40
0
(1) 0
(1a) -14
(TS1a) 46
(1b) 0
(TS1b) 76
(1c) 39
1.48
1.36
1.54
1.28
3.57
2.20
2.23
1.23
3.29
1.57
3.65
2.57
3.95
1.22
(ii)
Energy (kJ/mol)
40
0
-40
(1′) 0
(1a′) -27
(TS1a′) 42
58
(1b′) 6
(TS1b′) 54
(1c′) 27
25
Theoretical
Experimental

Figure 3

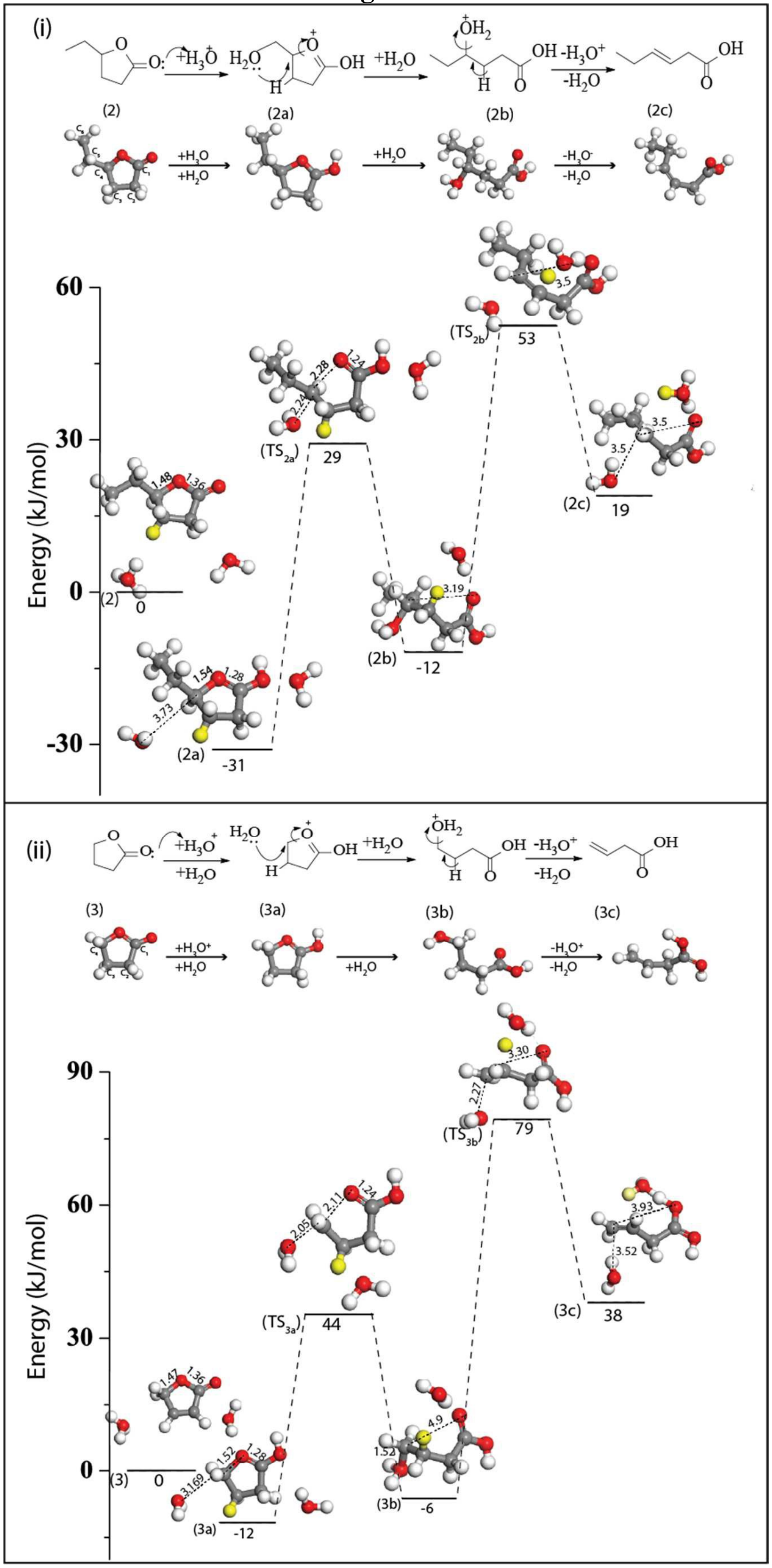
(i)
(2)
(2a)
(2b)
(2c)
$+H_3O^+$
$+H_2O$
$-H_3O^+$
$-H_2O$
C_1 C_2 C_3 C_4 C_5
Energy (kJ/mol)
60
30
0
-30
(2) 0
(2a) -31
(TS_{2a}) 29
(2b) -12
(TS_{2b}) 53
(2c) 19
1.48
1.36
1.54
1.28
3.73
2.28
2.24
1.24
3.19
3.5
3.5
3.5
(ii)
(3)
(3a)
(3b)
(3c)
90
60
30
0
(3) 0
(3a) -12
(TS_{3a}) 44
(3b) -6
(TS_{3b}) 79
(3c) 38
1.47
1.36
1.52
1.28
3.169
2.05
2.11
1.24
4.9
1.52
3.30
2.27
3.93
3.52

Figure 4

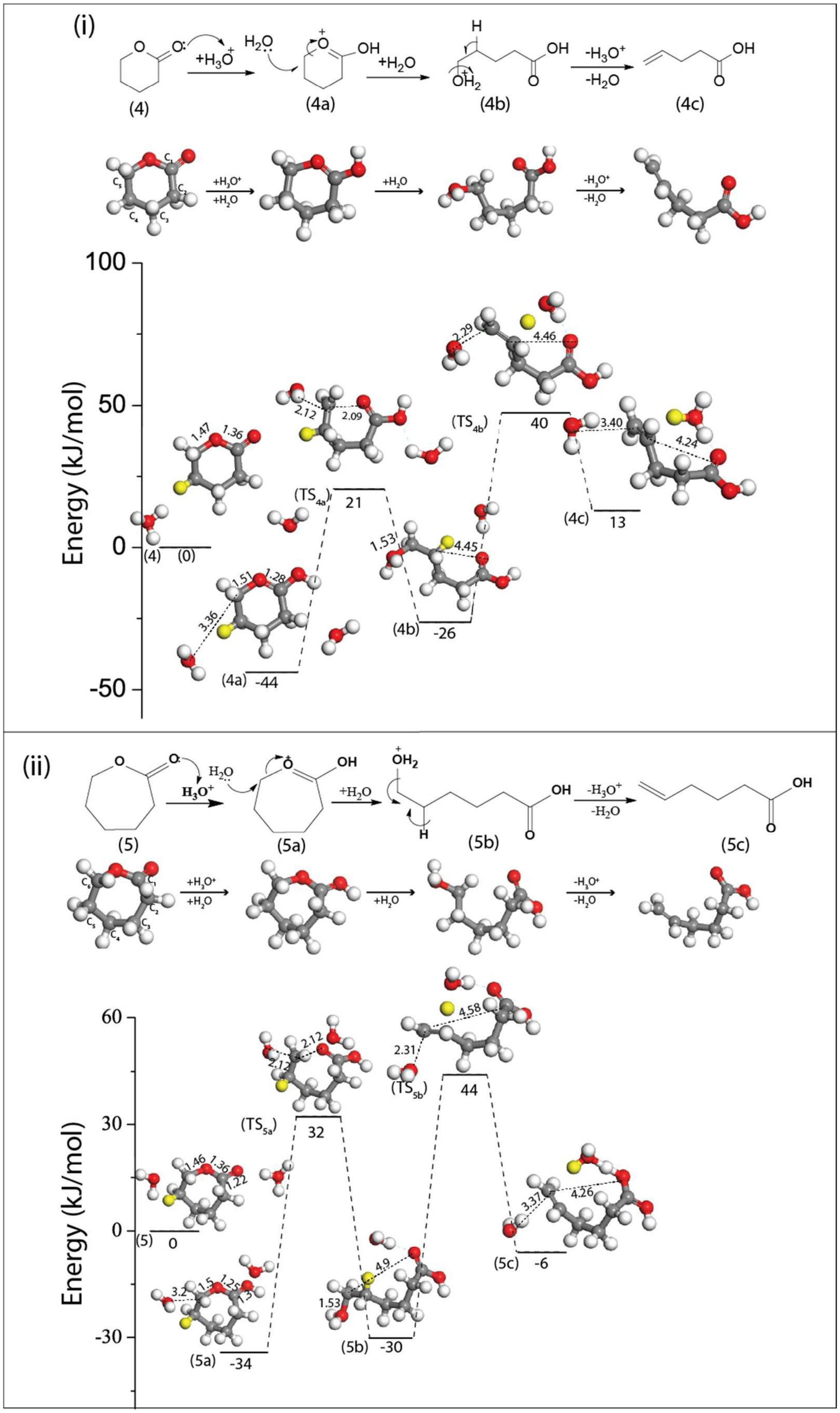
(i)
+H3O+
H2O
OH
+H2O
H
OH2
-H3O+
-H2O
(4)
(4a)
(4b)
(4c)
C1
C2
C3
C4
C5
+H3O+
+H2O
+H2O
-H3O+
-H2O
Energy (kJ/mol)
100
50
0
-50
(4)
(0)
1.47
1.36
(4a)
-44
1.51
1.28
3.36
(TS4a)
21
2.12
2.09
(4b)
-26
1.53
4.45
(TS4b)
40
2.29
4.46
(4c)
13
3.40
4.24
(ii)
H2O
H3O+
OH
+H2O
OH2
H
OH
-H3O+
-H2O
OH
(5)
(5a)
(5b)
(5c)
C1
C2
C3
C4
C5
C6
+H3O+
+H2O
+H2O
-H3O+
-H2O
Energy (kJ/mol)
60
30
0
-30
(5)
0
1.46
1.36
1.22
(5a)
-34
3.2
1.5
1.25
1.3
(TS5a)
32
2.12
2.12
(5b)
-30
4.9
1.53
(TS5b)
44
2.31
4.58
(5c)
-6
3.37
4.26

Figure 5

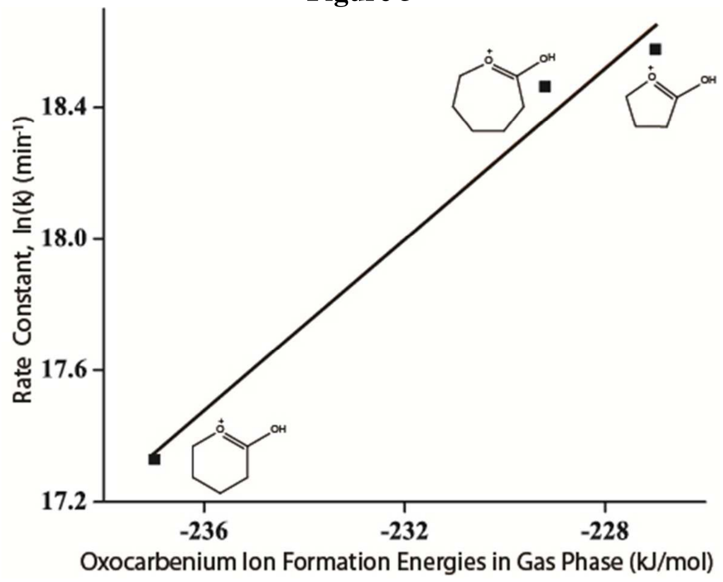
Rate Constant, ln(k) (min⁻¹)
18.4
18.0
17.6
17.2
-236
-232
-228
Oxocarbenium Ion Formation Energies in Gas Phase (kJ/mol)
O
OH
O
OH
O
OH

Figure 6

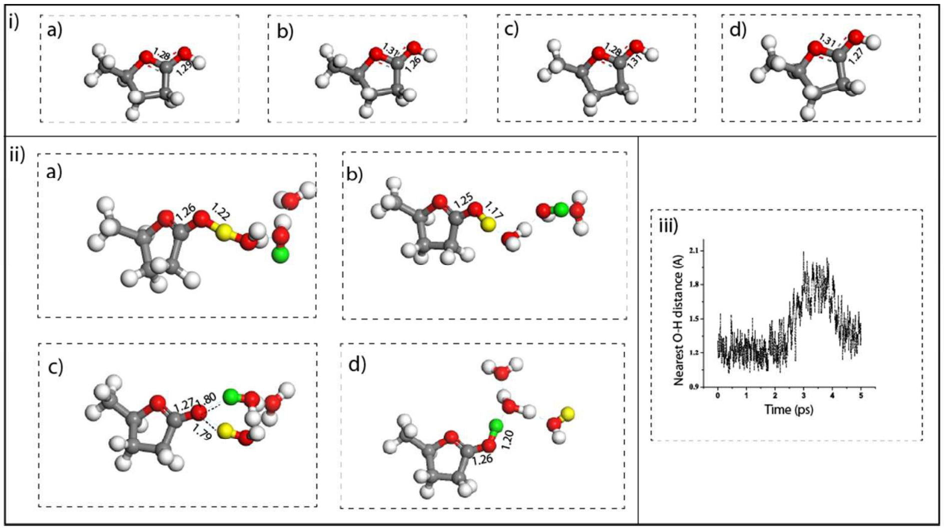
i)
a)
1.28
1.28
b)
1.31
1.26
c)
1.28
1.31
d)
1.31
1.27
ii)
a)
1.26
1.22
b)
1.25
1.17
c)
1.27
1.80
1.79
d)
1.20
1.26
iii)
Nearest O-H distance (A)
2.1
1.8
1.5
1.2
0.9
0
1
2
3
4
5
Time (ps)